Optik 127 (2016) 1438–1441

Contents lists available at ScienceDirect

Optik

journal homepage: www.elsevier.de/ijleo

Kinetics of LPP crystal nucleation and interface morphology studies

Xin Sun, Xiaojing Liu*, Xijin Xu, Ping Sun, Jinghua Guo

School of Physics and Technology, University of Jinan, Jinan 250022, Shandong Province, PR China

ARTICLE INFO

Article history:
Received 2 April 2015
Accepted 9 November 2015

Keywords:
Induction time
Nucleation kinetics
Growth from solutions
Metastable zone width
Atomic force microscopy

ABSTRACT

The nucleation parameters such as interfacial energy (γ), critical free energy (ΔG_{cr}), critical radius (r_{cr}) and critical nucleus number (n_{cr}) of LPP have been evaluated. Two types of growth patterns (spiral growth and nucleation at facet edges or corners) have been observed. Berg effect and impurity adsorption are responsible for the hopper or skeletal morphology. Step pinning can give rise to diffusion-field overlap in the face's center which can eventually lead to loss of stability of the step trains. The formation of line defect is linked to the embedding of microcrystals of the same phase as growth takes place. Ultimately, it can repair itself after multiple layers have grown.

1. Introduction

In the past decades, amino acids and their complexes based semiorganic materials were studied for different applications [1,2]. L-Prolinium phosphite (LPP) belongs to the orthorhombic crystal system with space group $P2_12_12_1$. Nucleation and growth kinetics give valuable information about the crystal growth process, which can be employed in the growth of large size crystals [3,4]. As per the available literature there is no systematic report available on growth kinetics of LPP. Thus, in the present study, we obtained the important nucleation properties, including solid-liquid interfacial energy, critical nucleation free energy and nucleus radius, by analyzing the primary nucleation process. This work also involved the characterization of the surface morphologies by atomic force microscopy (AFM) technique, which has been used extensively in recent years to characterize materials on nanometric and microscopic scale, based on their surface morphology, roughness, size distribution and micropore density [5].

2. Experimental

2.1. Solubility, metastable zone width and induction time measurements

The experiment was executed in different supersaturation ($S = C/C^*$) on 1.2, 1.3, 1.4, 1.5 and 1.6 at five different temperatures (27, 30, 35, 40 and 45 °C). Repeated trials were performed to ascertain the correctness of the observed results. After attaining the supersaturation at a given temperature, cooling was carried out until observation of the first crystal. The time taken for the formation of the first visible nuclei was very short and hence it was taken as the critical nuclei. The difference between the saturated temperature and the nucleation temperature is taken to be the metastable zone width of the system (Fig. 1). The solubility increases with an increase in temperature and nucleation temperature increases with the increase in concentration. The value of the metastable zone width depends not only on the temperature but also on the type of the crystal and its physicochemical properties. The study of induction time against supersaturation gives a guidance to control nucleation rate for developing good quality single crystals. Different methods are used for the measurement of induction time. Conductivity and turbidity methods are more suitable for materials having low solubility whereas dilatometer and direct vision methods are suitable for materials having moderate solubility and in the present work, the direct vision observation method was used to measure the induction time.

2.2. AFM investigations

By using the optical microscopy, good quality and optically transparent crystals without visible defects were selected. AFM experiments were carried out using a Nanoscope, IIIa dimension 3100 AFM instrument of Digital Instruments Incorporation. All images were recorded in contact mode using Si_3N_4 cantilevers (NP-10, Veeco Probes) with a nominal spring constant of 0.58 N/m.

---

* Corresponding author. Tel.: +86 531 8276 5480; fax: +86 531 8276 5480.
E-mail address: lxj@mail.sdu.edu.cn (X. Liu).

http://dx.doi.org/10.1016/j.ijleo.2015.11.028
0030-4026/© 2015 Elsevier GmbH. All rights reserved.

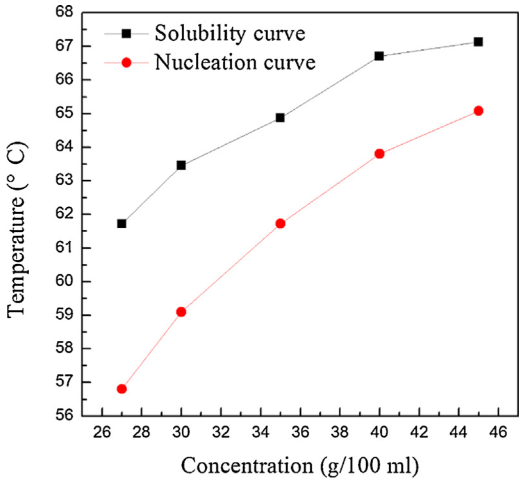

Fig. 1. Metastable zone width of LPP as a function of temperature.

Image processing and analysis were performed using Spiwin (3.01 version) software pre-installed to the AFM system.

3. Nucleation theoretical background

The steady-state crystal nucleation rate is given by the classical Volmer's relation [6]

$$J = A\exp\left(\frac{-G_{cr}}{k_BT}\right) \tag{1}$$

For homogeneous crystal nucleation, ΔG_{cr} (the energy barrier for nucleation), assuming spherical nuclei, is proportional to $\Delta\mu = k_B\mathrm{T}\ln S$ in power minus two:

$$\Delta G_{cr} = \frac{16\pi}{3}\frac{\Omega^2\gamma^3}{\Delta\mu^2} = \frac{16\pi\Omega^2\gamma^3}{3k_B^2T^2\ln^2 S} \tag{2}$$

with Ω denotes the molecular volume, γ being its specific interfacial energy. Thus, the radius of the critical nucleus (r_{cr}) is expressed as

$$r_{cr} = \sqrt{\frac{3\Delta G_{cr}}{4\pi\gamma}} = \frac{2\Omega\gamma}{k_BT\ \ln S} \tag{3}$$

After substitution of Eq. (2) into Eq. (1), the logarithmic form of the relationship between t_{ind} and S can be expressed as

$$\ln t_{ind} = -\ln A + \frac{16\pi\Omega^2\gamma^3}{3k_B^3T^3}\frac{1}{\ln^2 S} \tag{4}$$

The plot of $\ln t_{ind}$ against $1/(\ln S)^2$ line with a slope of α is calculated as

$$\alpha = \frac{16\pi\Omega^2\gamma^3}{3k_B^3T^3} \tag{5}$$

Therefore, the interfacial energy is evaluated from

$$\gamma = \left(\frac{3\alpha k_B^3T^3}{16\pi\Omega^2}\right)^{1/3} \tag{6}$$

In addition, the so-called nucleation theorem renders the size of the critical nucleus n_{cr} (in terms of the number of molecules constituting it) [7,8]:

$$n_{cr} = k_BT\frac{d(\ln J)}{d(\Delta\mu)} = \frac{d(\ln J)}{d(\ln S)} = \frac{32\pi\Omega^2\gamma^3}{3(k_BT\ \ln S)^3} \tag{7}$$

The possibilities to calculate the value of ΔG_{cr}, r_{cr} and n_{cr} show why knowledge of the steady-state crystal nucleation rate (J) is very useful from a practical point of view.

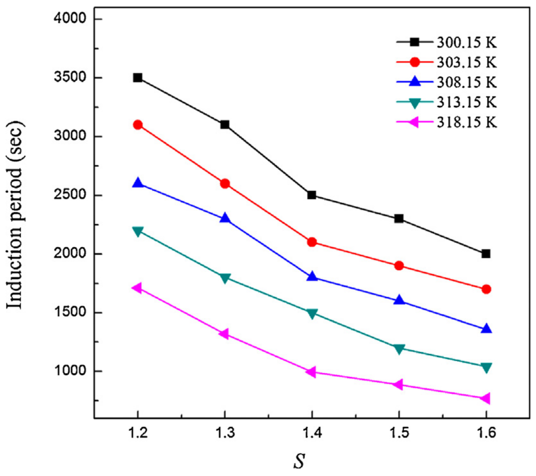

Fig. 2. Induction time versus supersaturation ratio.

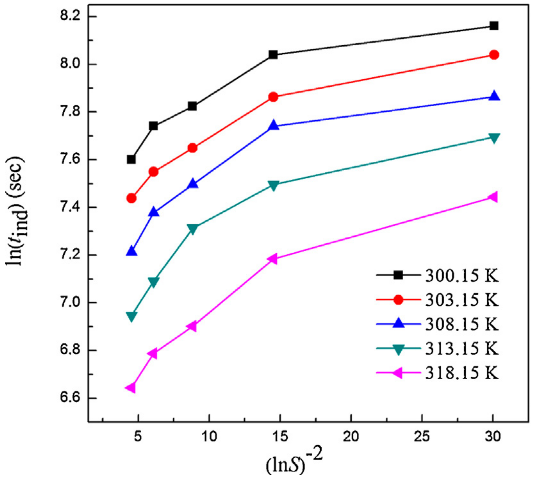

Fig. 3. Plot of $(\ln S)^{-2}$ versus $\ln(t_{ind})$ at various temperature.

4. Results and discussion

As the supersaturation is increased (Fig. 2), the induction time is decreased which indicate the increase of nucleation rate. From Fig. 3, interfacial energy at different temperatures are estimated to be $\gamma_{300.15\ \mathrm{K}} = 1.18\ \mathrm{mJ/m^2}$, $\gamma_{303.15\ \mathrm{K}} = 1.24\ \mathrm{mJ/m^2}$, $\gamma_{308.15\ \mathrm{K}} = 1.28\ \mathrm{mJ/m^2}$, $\gamma_{313.15\ \mathrm{K}} = 1.36\ \mathrm{mJ/m^2}$ and $\gamma_{318.15\ \mathrm{K}} = 1.43\ \mathrm{mJ/m^2}$, respectively. A lower value of interfacial energy represents the higher growth rate and solute can easily crystallize from solution. Based on the experimentally found interfacial energy values, the various nucleation parameters such as ΔG_{cr}, r_{cr} and n_{cr} can be calculated (Fig. 4). With the increase in the supersaturation at the same temperature, the critical nucleus radius decreases from 8.07 Å to 2.75 Å for supersaturation range 1.2–1.6. That means the formation of critical nucleus will be increased which may results in spurious nucleation. The same trend prevails for the critical free energy and number of the critical nucleus. Moreover, as temperature increases, there is a marked drop in the critical nucleus radius and the critical free energy at the same level of supersaturation. The higher the temperature is, the faster the decline. It is consequently interpreted that the enhancement of temperature or supersaturation makes the nucleation easier when one parameter is fixed.

As shown in Fig. 5(a), the spiral centers are of the composite type, with multiple dislocations located close to each other and generating multiple steps. It is well-known that the formation of composite